# Diffusion Weighted Imaging of Human Prostate at 3T: Evaluation of Diffusion and Microperfusion Contributions.

**P. Vermathen[1], T. Binser[1], C. Boesch[1], and H. C. Thoeny[2]**

[1]Dept. Clinical Research, University & Inselspital, Bern, Switzerland, [2]Dept. Radiology, University & Inselspital, Bern, Switzerland

**Introduction:** Diffusion weighted imaging (DWI) of the human prostate has been shown to be of clinical interest for tumor detection [1-3]. However, only very few diffusion studies have been reported in human prostate at a field strength of 3T or higher [4,5]. It is well known that in DWI measurements in addition to diffusion, microperfusion may contribute to the signal decay at low b-values and its analysis may provide additional information, provided that the two entities can be separated. However, although some studies have recognized and taken care of this effect [3,4] to our knowledge only one recent abstract has tried to separate diffusion and microperfusion contributions at 1.5T [6]. Following up on that study we performed DWI in the prostate of healthy subjects. The main goal was to establish a protocol for reliable determination of diffusion parameters at 3T, including apparent diffusion coefficients (ADCs), and analysis of micro-perfusion contributions.

**Methods:** Eight healthy subjects (mean age: 39y, range: 24-64y) were measured on a 3T MR scanner (Trio, Siemens) using a 6-channel body coil. After morphological imaging, transverse (4 subjects) and/or coronal (6 subjects) diffusion–weighted multisection single shot echo-planar imaging was performed, applying parallel imaging (SENSE, acceleration factor of 3). Ten diffusion gradient b-values were applied (b=0, 10, 20, 50, 100, 200, 300, 500, 700, 1000 sec/mm$^2$), The following parameters were used: 6 averages and 3 orthogonal gradient directions, TR=2.8s, TE=67ms, FOV: 40cm, 11 slices, slice thickness 5mm, intersection gap 1mm, matrix size 128×128, scan time ~8min. Processing was performed by I) monoexponential fitting, yielding $ADC_T$, and II) biexponential fitting, yielding $ADC_D$ (mostly determined by diffusion) and the contribution of the fast decaying component ("perfusion fraction", $F_P$). ROIs were selected in right and left central gland (CG) as well as in tissue surrounding the urethra (UD), and in several areas of the peripheral zone (PZ).

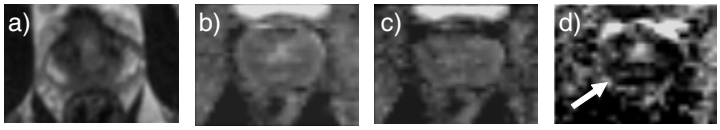


Fig. 1: Morphological MRI (a) and maps from an axial diffusion scan: b) $ADC_T$, c) $ADC_D$, d) $F_P$.

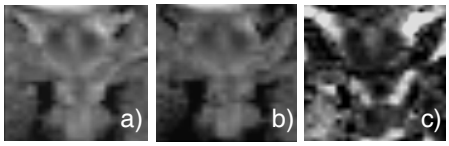


Fig. 2: Maps from a coronal diffusion scan: a) $ADC_T$, b) $ADC_D$, c) $F_P$.

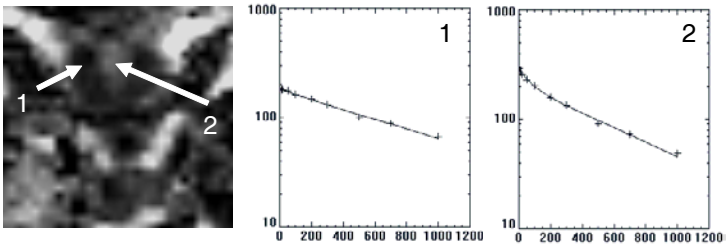


Fig. 3: $F_P$-map (as in Fig. 2c). The arrows indicate the ROI positions for the plots of the signal decay with increasing b-values.

**Results:** Although geometric distortions that are commonly observed in EPI-based sequences at higher field strength were relatively low (Fig. 1), due to parallel imaging allowing for short TE times, they prevented the use of morphological images as anatomical guidance for ROI selection. Therefore, ROIs were drawn on the EPI image with b=0 sec/mm$^2$. The $ADC_D$ and $ADC_T$ maps demonstrated good contrast between different anatomical regions, and for the majority of subjects also the $F_P$-maps provided useful information (Figs.1, 2). Generally, the $F_P$-maps demonstrated higher signal intensity in UD than in the surrounding tissue in CG. The plots in Fig. 3 demonstrate the good linear correlation (ln(Intensity) vs. b-values in ROIs from CG, while for ROIs from UD the decay is clearly biexponential.

$ADC_T$ values were comparable to previously published values and were significantly smaller in CG than in PZ (Table 1), though the difference between the values was greater than has been reported. $ADC_T$ in tissue surrounding the urethra was significantly higher than in the right and left central gland. $ADC_D$ values were significantly lower than $ADC_T$ in all three analyzed regions. Similar to $ADC_T$, $ADC_D$ was significantly lower in CG than in UD and in PZ, in contrast to the previous study [6]. This different finding may be due to the lower number of subjects in our study or due to careful exclusion of UD (with higher $ADC_D$), when placing the ROI in the central gland. $F_P$ was low in the central gland excluding the urethra, while $F_P$ was significantly higher in PZ. However, determination of $F_P$ in PZ was much less reliable as evidenced by the much greater individual variance of the analyzed ROIs. The significantly higher $F_P$ in PZ may therefore be spurious.

**Discussion:** The results of this study demonstrate that the determination of $F_P$ from DWI in prostate provides useful information in addition to the ADC values. $F_P$ can be determined quite reliably in CG and helps to exclude areas containing the urethra. However, analysis of $F_P$ in PZ must be interpreted carefully, because of possible spurious contributions from the edge of the prostate (see arrow in Fig. 1d). However, since $ADC_T$ includes microperfusion components, detection of these artifacts by investigating the signal decay with increasing b-values for suspicious ROIs may also prevent a false $ADC_T$ estimation. This is important because an unambiguous assignment of PZ from the EPI image is sometimes difficult.

| | $ADC_T$ | $ADC_D$ | $F_P$ |
|---|---|---|---|
| **UD** | 164±19 | 145±20 | 0.16±0.07 |
| **CG** | 127±16 | 117±15 | 0.09±0.02 |
| **PZ** | 187±30 | 163±37 | 0.19±0.06 |

**Table 1:** Mean values for ADC (×10$^{-5}$ mm$^2$/sec) and FP in different tissue types.

**References**

1. Gibbs P, Tozer DJ, Liney GP, Turnbull LW. Magn Reson Med 46**:**1054 (2001)
2. Sinha S, Sinha U. Magn Reson Med 52**:**530 (2004)
3. Issa B. J. Magn Reson Imaging 16**:**196 (2002)
4. Pickles MD, Gibbs P, Sreenivas M, Turnbull LW. J. Magn Reson Imaging 23**:**130 (2006)
5. Miao H, Fukatsu H, Ishigaki T. Eur. J. Radiol. Article in Press (2006)
6. S. F. Riches, K. Hawtin, N. M. deSousa, Proc. ISMRM 14: 87 (2006).

**Acknowledgment:** This work was supported by SNF (National Center of Competence in Research "Computer-aided and image-guided medical interventions") and by SNF 320000-111959.